Conf-820635--5

BNL 31584

BNL--31584

DE82 018060

S = −2 DIBARYONS AND HYPERNUCLEI*

C. B. Dover

Brookhaven National Laboratory
Upton, New York, USA 11973

* Invited talk at the International Conference on Hypernuclear and Kaon Physics, June 20-24, 1982, Heidelberg, Germany.

The submitted manuscript has been authored under contract DE-AC02-76CH00016 with the U.S. Department of Energy. Accordingly, the U.S. Government retains a nonexclusive, royalty-free license to publish or reproduce the published form of this contribution, or allow others to do so, for U.S. Government purposes.

S = -2 DIBARYONS AND HYPERNUCLEI

C. B. Dover

Brookhaven National Laboratory, Upton, New York, USA

ABSTRACT

Future prospects for the exploration of doubly strange hypernuclear systems are evaluated. Such systems may be produced via the double strangeness exchange reactions (K^-,K^+) or (K^-,K^o) on nuclear targets. Theoretical estimates are given of the formation cross sections for Ξ^- hypernuclear states via the one-step $K^-p \to K^+\Xi^-$ process, or discrete states of the $\Lambda\Lambda$ hypernucleus in the two step reaction $K^-p \to \pi^o\Lambda$ followed by $\pi^o p \to K^+\Lambda$. Recently, there has been much discussion of six quark (dibaryon) states in the Bag Model. Arguments are given which indicate that the (K^-,K^+) reaction on light nuclear targets (ex. ^{3}He) affords a very promising way of producing the lowest-lying S = -2 dibaryon (called the H).

I. INTRODUCTION

The spectroscopy of strangeness S = -1 hypernuclei (Λ and Σ) has received much attention over the past decade (1). In contrast, the properties of nuclear systems of strangeness -2 are essentially unexplored. A few candidates for $\Lambda\Lambda$ and Ξ^- hypernuclear events exist in the emulsion data (2, 3) but these systems have not been looked for in modern experiments with magnetic spectrometers, which have focussed on studies of the (K^-,π) reaction. In this paper, strong motivation is provided to look for bound states of S = -2 systems, in the form of Ξ or $\Lambda\Lambda$ hypernuclei or stable six quark states.

The simplest S = -2 systems beyond the $\Xi(1321)$ or $\Xi^*(1530)$ are dibaryons. Quark bag models (4) predict a variety of six quark states with different strangeness. There has been intense discussion on the existence of S = 0 dibaryon resonances in nucleon-nucleon scattering (5), as well as possible S = -1 dibaryons seen in the Λp system (6). In both cases, the proposed six-quark bag states are unstable with respect to strong decay. This gives rise to difficult questions of interpretation, since one must distinguish between a true dibaryon signal and a threshold enhancement produced as a coupled channel effect ($NN \leftrightarrow \Delta N$ for S = 0, $\Lambda N \leftrightarrow \Sigma N$ for S = -1). The situation is potentially more favorable in the S = -2 sector, where the Bag Model predicts (7) a dibaryon (the H, with quark composition $(uuddss)_{0^+,I=0}$) which is stable against strong decay. The H plays a special role in multiquark ($n > 3$) spectroscopy, since it is the only such object which is predicted to decay weakly. In addition, it cannot be confused with a deuteron-like non-relativistic bound state, since it is supposed to be strongly bound (80 MeV or more) with respect to the $\Lambda\Lambda$ threshold. Here, we provide some estimates of the cross section for the reaction $^3He(K^-,K^+)nH$, which indicate that this process offers a most promising tool for H production.

The $(K^-,K^{+,o})$ reactions on nuclear targets provide a window on the spectroscopy of Ξ and $\Lambda\Lambda$ hypernuclear states. We argue here that such studies represent one logical next step in the evolution of hypernuclear physics (another important step would be the high resolution study of S = -1 hypernuclei). The new spectroscopy of Ξ and $\Lambda\Lambda$ hypernuclei is rich, although only a restricted portion of these states (high spin states with no spin flip) are excited with measurable cross sections in the high momentum transfer (K^-,K) reaction. One goal of these studies would be to extract information on the single particle properties of a Ξ in the nucleus, i.e. the real and imaginary well depths and the one-body spin-orbit potential. Recently, narrow Σ-hypernuclear states have been observed (8). As we indicate here, narrow Ξ states are also likely to exist; their widths depend delicately on the hypernuclear wave functions as well as the (essentially unknown) rate for the $\Xi N \to \Lambda\Lambda$ conversion process. One might also ultimately hope to learn something about the $\Lambda\Lambda$ and ΞN residual interactions, which would be useful in extending our knowledge of the SU(3) structure of baryon-baryon forces.

II. Ξ HYPERNUCLEI

The spectroscopy and production cross sections expected for Ξ hypernuclei are discussed in some detail in a recent paper by Dover and Gal (9), which is summarized in skeletal form here.

In the emulsion data, there are about seven events which are candidates for interpretation in terms of Ξ hypernuclear formation (10). The species tentatively identified ranged from $^{8}_{\Xi}He$ to $^{30}_{\Xi}Mg$. Except for the $^{30}_{\Xi}Mg$ event, the Ξ binding energy B_{Ξ} displays a smooth mass dependence, which can be reproduced with a phenomenological potential $V_{\Xi}(r)$ of the form

$$V_{\Xi}(r) = -V_{o\Xi}\left(1 + \exp((r-R)/a)\right)^{-1} \quad (1)$$

Assuming $R = r_0 A^{1/3}$, with $r_o = 1.1$ fm and $a = 0.65$fm, we obtain the Ξ well depth $V_{o\Xi} \gtrsim 24 \pm 4$ MeV. Theoretical predictions (11) based on the SU(3) potential model of deSwart et al. (12) give $V_{o\Xi} \approx 23$ MeV (Model D) or -28 MeV (Model F). Thus, if the Ξ emulsion data are taken seriously, Model F of deSwart et al. (12) is strongly disfavored, since it predicts a repulsive Ξ potential. Using the potential of Eq. (1), one may now generate the spectrum of anticipated Ξ single particle states in a variety of nuclei. The results are shown in Fig. 1. These are the bound Ξ states that one would populate in the (K^-,K^+) reaction on ^{12}C, ^{16}O, ^{28}Si and ^{40}Ca targets, respectively; the resulting ΞN^{-1} particle-hole states would acquire a spreading width Γ_{Ξ} due to the strong conversion process $\Xi^- p \to \Lambda\Lambda$. No data exists on this reaction in the momentum region (≤300 MeV/c) of interest. Estimates of Γ_{Ξ} have been based on a K and K* exchange model for $\Xi^- p \to \Lambda\Lambda$ (9). This yields rough estimates of $\Gamma_{\Xi} \gtrsim 10$ MeV for s-states and 5 MeV or so for Ξ states near threshold. For particular Ξ configurations, the optical model estimates of Γ_{Ξ} may be substantially modified due to the spin-isospin selectivity of the $\Xi^- p \to \Lambda\Lambda$ process, i.e., at low momentum, it can proceed only via the ^1S_o, I = 0 channel. Such an effect has been discussed for Σ hypernuclei (13), where the analogous reaction $\Sigma^- p \to \Lambda n$ goes predominantly through the $^3S_1$, I = 1/2 channel.

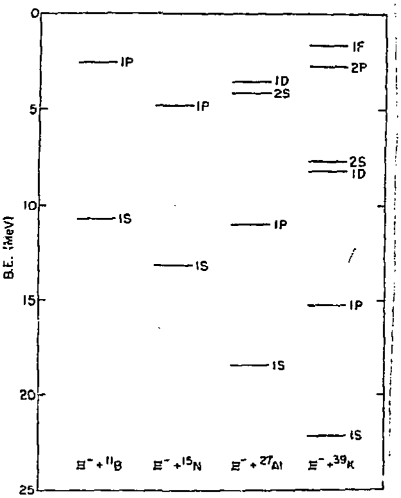

Fig. 1. Single particle states for the Ξ

Various schemes may be envisaged for making Ξ hypernuclei: a) produce a beam of fast Ξ particles, degrade them in energy, and look for capture of slow Ξ's in nuclei; b) look for the direct one step production of a Ξ-nuclear state in the (K^-,K^+) or (K^-,K^o) reaction; c) the use of multi-body final states, such as $(K^-,K\pi)$, to produce a lower momentum Ξ. Methods b) and c) have been examined in ref. (9). The $(K^-,K\pi)$ channel does not appear to be very promising, since the produced Ξ is still not slow, and the problems of detection efficiency and resolution are more severe. The momentum transfer Q(0°) for a K^+ at 0° is shown in Fig. 2 as a function of K^- lab momentum, both for proton and heavy nuclear targets. For a wide range of p_{lab}, we see that Q(0°) for the (K^-,K^+) reaction on a nucleus is somewhat larger than the Fermi momentum, hence leading to the population of <u>high spin</u> ΞN^{-1} states.

The rates for the formation of Ξ hypernuclear states in (K^-,K^+) are proportional to the elementary $K^- p \to K^+ \Xi^-$ cross section. The available information is summarized in Fig. 3, taken from ref (9); the data is averaged over the small angle region for the K^+, including a factor α which accounts for the kinematic transformation from the two-body to many-body lab systems. The forward $K^- p \to K^+ \Xi^-$ lab cross section displays a peak in the region of $p_{lab} \gtrsim 1.8$ GeV/c. Since Q(0°) varies slowly in this region, as per Fig. 2, the (K^-,K^+) cross sections to discrete ΞN^{-1} hypernuclear states just follow the momentum dependence of the elementary process. For ^{12}C and ^{28}Si targets, the forward lab differential cross sections for the (K^-,K^+) reaction, leading to ΞN^{-1} states in $^{12}_{\Xi}Be$ and $^{28}_{\Xi}Mg$, are shown in Fig. 4.

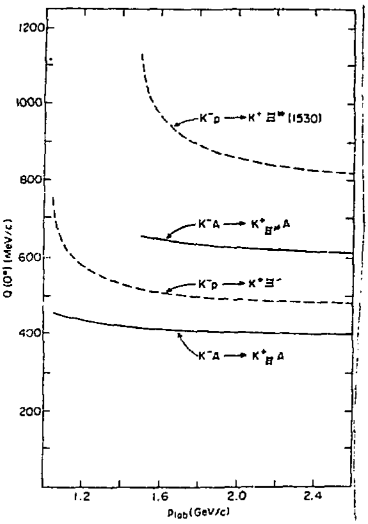

Fig. 2. Momentum transfer for Ξ production.

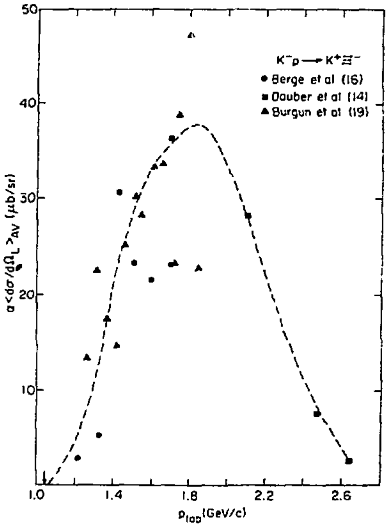

Fig. 3. Forward cross section for Ξ production

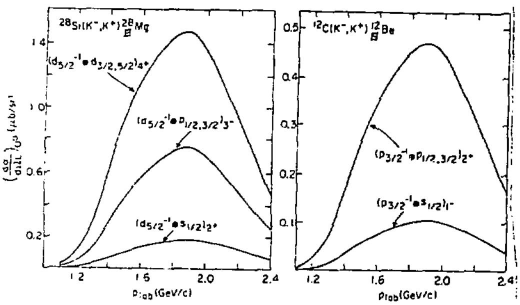

Fig. 4. Forward cross sections for discrete Ξ-hole states

The preference for high spin states is evident. Even for the highest spin bound states shown, the reaction is mismatched, i.e. the cross section drops monotonically with angle. In the region of 1.8 GeV/c, the cross sections to ΞN^{-1} states are predicted to be as large as 1 μb/sr; since kaon beam intensities at this momentum are much larger than at 800 MeV/c, where (K^-,π^-) experiments are typically done, such cross sections should be accessible experimentally. High resolution is not required, since the Ξ spreading width is presumably of the order of a few MeV or more.

III. ΛΛ HYPERNUCLEI

Double Λ hypernuclei may be formed in the (K^-,K^+) or (K^-,K^0) reactions via two-step processes $\bar{K}N \to \pi\Lambda$ followed by $\pi N \to K\Lambda$ or $\bar{K}N \to K\Xi$ plus $\Xi N \to \Lambda\Lambda$. These two mechanisms are expected to be well separated kinematically. As we saw in II, the $\bar{K}N \to K\Xi$ process peaks around 1.8 GeV/c, while $\pi N \to K\Lambda$ is maximal at a much lower pion momentum about 1.02 GeV/c, corresponding to a kaon momentum of 1.1 GeV/c. We concentrate on this latter process here, providing estimates of (K^-,K^+) cross sections for discrete ΛΛ hypernuclear states. Earlier estimates focussed on sum rules (14), which indicated that most of the (K^-,K^+) strength (a few μb/sr) went into the quasielastic part of the ΛΛ spectrum (because of the sizable momentum transfer). Here we concentrate on the very small cross sections (a few nb/sr) to discrete ΛΛ states.

To estimate the ΛΛ cross sections via the two-step process $K^-p \to \pi^0\Lambda$, $\pi^0 p \to K^+\Lambda$, we have adapted (15) the coupled channel code (16) CHUCK to the present situation. Back coupling is neglected, so our results are equivalent to second order DWBA. Full distortions of the K^-, π^0, and K^+ waves are included, using optical potentials of Woods-Saxon shape which are adjusted to reproduce the available scattering data for K's and π's on ^{12}C at 800 MeV/c (17). Bound state wave functions for protons and Λ's in a Woods-Saxon potential are used to generate transition form factors; the parameters of the well are adjusted to reproduce the appropriate separation energies.

As typical examples, the reactions $^{16}O(K^-,K^+)^{16}_{\Lambda\Lambda}C^*$ and $^{40}Ca(K^-,K^+)^{40}_{\Lambda\Lambda}Ar^*$ have been investigated at 1.1 GeV/c. As for the Ξ hypernuclei, the highest spin states of the $\Lambda\Lambda$ hypernucleus are preferentially populated in the (K^-,K^+) reaction, since the momentum transfer is of order 400 MeV/c, even at 0°. Some of the states expected in $^{16}_{\Lambda\Lambda}C$ are shown in Fig. 5. We indicate only natural parity states obtained by coupled $(s_\Lambda s_\Lambda)_{L=S=0}$, $(s_\Lambda p_\Lambda)_{L=1,S=0}$ or $(p_\Lambda p_\Lambda)_{L=2,S=0}$ $\Lambda\Lambda$ pairs to the 0^+ ground state of the ^{14}C core and the 2^+ core excited state at about 7-8 MeV. The latter state in ^{14}C is particularly relevant in a weak coupling picture of $^{16}_{\Lambda\Lambda}C$, since in the shell model it is a relatively pure two-hole state, i.e. $^{16}O(g.s.) \otimes (p_{3/2}^{-1}p_{1/2}^{-1})_{L=2,S=0}$. The other low lying core states in ^{14}C are dominantly of 3 hole-1 particle or 4 hole-2 particle character with respect to ^{16}O, and do not enter in the weak coupling limit considered here. The highest spin bound state of $^{16}_{\Lambda\Lambda}C$ which would be populated in the (K^-,K^+) reaction is the 4^+ configuration of structure $^{14}C(2^+) \otimes (p_\Lambda p_\Lambda)_{L=2,S=0}$. Note that the spin-flip amplitudes for both $\bar{K}N \to \pi\Lambda$ and $\pi N \to K\Lambda$ are rather unimportant, so we consider only natural parity states in the intermediate nucleus $^{16}_{\Lambda}N$ and $S = 0$ $\Lambda\Lambda$ pairs in $^{16}_{\Lambda\Lambda}C$. The possible routes to 4^+ final states for the two-step (K^-,K^+) process which we consider are shown in Fig. 6. Each transition is labelled by the orbital angular momentum transfer ΔL, which also equals ΔJ (since $\Delta S=0$). The transition to the $p_\Lambda p_\Lambda$ final state is seen to proceed in two successive $\Delta L=2$ transitions via $(p_\Lambda p^{-1})_{2^+}$ states in $^{16}_{\Lambda}N$. Since the $\bar{K}N \to \pi\Lambda$ process has low momentum transfer q at 0° and $\pi N \to K\Lambda$ has high q, a different sharing of the total angular momentum change $\Delta J = 4$ can lead to a kinematic enhancement of the (K^-,K^+) cross section. An example is given in Fig. 6, where $\Delta L = 1$ followed by $\Delta L = 3$ leads to a 4^+ state of the form $^{14}C(2^+) \otimes (s_\Lambda d_\Lambda)_{L=2,S=0}$. The differential 0° cross sections to the two 4^+ states are shown in Fig. 7. Even though the d_Λ is a continuum state (here taken to be artificially bound by 0.1 MeV, with a very large r.m.s. radius), the cross sections to the $p_\Lambda p_\Lambda$ and $s_\Lambda d_\Lambda$ 4^+ states are comparable, of the order of several nb/sr. In an oscillator potential, the $s_\Lambda d_\Lambda$ configuration would have the same energy as $p_\Lambda p_\Lambda$. For a more realistic Woods-Saxon potential of depth $V_{0\Lambda} \approx 30$ MeV, the d_Λ single particle resonance lies more than 10 MeV in the continuum and is very broad (Γ>10 MeV). Thus the 4^+ state in $^{16}_{\Lambda\Lambda}C$ arising from $s_\Lambda d_\Lambda$ would generate a smooth background spread over a broad range of excitation energies above the

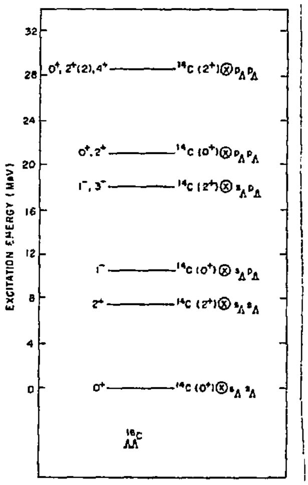

Fig. 5. Natural parity levels in $^{16}_{\Lambda\Lambda}C$

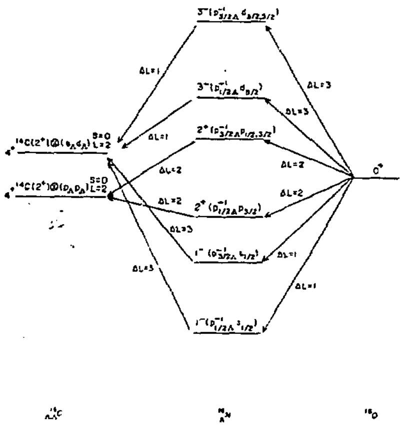

Fig. 6. Routes from the 0^+ target ^{16}O to the 4^+ states in $^{16}_{\Lambda\Lambda}C$

$p_\Lambda p_\Lambda$ 4^+ state, which is particle stable (p_Λ is bound by about 3 MeV here). In Fig. 7, we also show the (K^-,K^+) cross sections to other selected states in ${}^{16}_{\Lambda\Lambda}C$. The cross sections to lower spin states of type $(s_\Lambda d_\Lambda)$ and $(p_\Lambda p_\Lambda)$ are much less than those to "stretch states". Note that one can populate unnatural parity states in ${}^{16}_{\Lambda\Lambda}C$ at $\theta \neq 0°$, even in the absence of spin flip in either of the two-body reactions, but the cross sections are negligible. The (K^-,K^+) cross section to the ${}^{16}_{\Lambda\Lambda}C$ ground state is also seen to be small (low spin). In Fig. 8, we display the (K^-,K^+) excitation function at 0°. We include the ${}^{16}_{\Lambda\Lambda}C$ states of Fig. 5. The largest cross section to a $\Lambda\Lambda$ bound configuration goes to the 3^- state. The strength associated with the continuum $s_\Lambda d_\Lambda$ configuration has been spread over about 15 MeV, roughly the escape width of the d_Λ. The other states are provided with a width of 2 MeV, to account for experimental resolution.

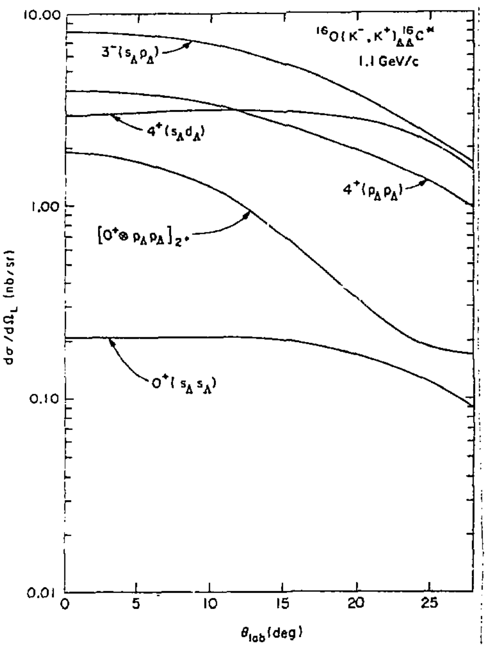

Fig. 7. (K^-,K^+) cross sections to selected states in ${}^{16}_{\Lambda\Lambda}C$

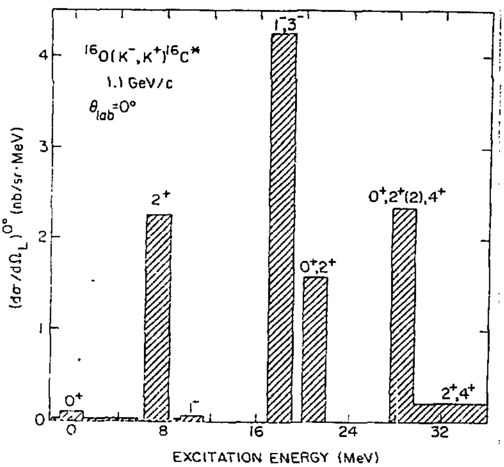

Fig. 8. Excitation function at 0° for ${}^{16}O(K^-,K^+){}^{16}_{\Lambda\Lambda}C$ at 1.1 GeV/c

We have made some attempts (15) to determine an optimum target for (K^-,K^+) reactions, in order to provide the best matching of ΔJ and q. In addition to ${}^{16}O$, another good example seems to be ${}^{40}Ca$. In this mass region, the d_Λ single particle state is just bound (by ~ 1 MeV), so one can have successive $d \to d_\Lambda$ transitions to particle stable states in ${}^{40}_{\Lambda\Lambda}Ar$. In the shell model, the ${}^{38}Ar$ core has a 4^+ excited state which has a sizable component of ${}^{40}Ca \otimes (d^{-1}d^{-1})_{L=4,S=0}$. In the weak coupling picture, we obtain a high spin 8^+ state by coupling a $(d_\Lambda d_\Lambda)_{L=4,S=0}$ pair to this 4^+ core state. The (K^-,K^+) cross section to this state is of the order of a few nb/sr, as for an ${}^{16}O$ target.

IV. THE H DIBARYON

The spectroscopy of multiquark states is a very intriguing subject. Quark "molecules" with more complicated structures than QQQ or $Q\bar{Q}$ have often been discussed theoretically and searched for experimentally, for instance $Q^2\bar{Q}^2$ "baryonium" states, $Q^4\bar{Q}$ Z^* resonances, and Q^6 dibaryon states. The Q^6 states come with various values of strangeness. For S=0 and S = -1, many states have been predicted, and some experimental candidates exist (4-6). The problem is that all of these Q^6 states have strong decay channels available, and so it is difficult to disentangle multiquark bag states from cross section enhancements due to coupled channel effects near thresholds. This is true for structures seen in NN scattering near the $N\Delta$ threshold and in the Λp system near the ΣN thresholds. The S = -2 sector is unique, in that it offers a candidate for a six quark state which is stable against strong decay. This particle, the H, was first proposed by Jaffe (7). It has quantum numbers $J^\pi = 0^+$, I = 0, and a predicted mass some 80 MeV below the $\Lambda\Lambda$ threshold, around $m_H = 2150$ MeV. The quark composition of the H is uuddss, with all six quarks in the lowest s-state. Such an object could be formed by a fusion of two three-quark bags, without the need for any quarks to be promoted to higher orbitals (for NN, in contrast, some quarks must be pushed up to the p-state to satisfy the Pauli principle in the six quark bag). Clearly, the fact that all quarks occupy s-states in the H contributes to its appreciable "condensation energy" with respect to two Λ's. As an amusement, one might also imagine other stable multiquark objects of this type, an example being a "Noah's Ark" particle with all quark species present in pairs: $(\text{uuddssttbbcc})_{0^+,I=0}$.

One might ask whether an object with the quantum numbers of the H can be produced in ordinary potential models. Using the SU(3) model of deSwart et al. (12), one can construct $\Lambda\Lambda$ and Ξ^-p potentials from various meson exchanges in the $^1S_0$,I=0 channel (18). Because of the absence of a one pion exchange term, the attractive potentials in this channel (or any other) are not sufficient to support any S = -2 bound state. Thus the H, if it exists, is clearly not a non-relativistic two-body bound state.

The weak decay modes available to the H depend on its mass. For $m_N+m_\pi+m_\Lambda<m_H<2m_\Lambda$ (2195 MeV < m_H < 2230 MeV), the channel $H \to \Lambda N\pi$ is open, so τ_H is presumably of order 10^{-10} sec ($\sim\tau_\Lambda$). If $m_\Sigma + m_N < m_H < m_N + m_\pi + m_\Lambda$ (or 2130 to 2195 MeV), then the modes $H \to \Sigma^-p$, Σ^0n, and Λn prevail. For $m_\Lambda + m_N < m_H < m_\Sigma + m_N$ (2055 to 2130 MeV), only $H \to \Lambda n$ is left among the YN decays. Finally, if $2m_n < m_H < m_\Lambda + m_N$, only the doubly weak mode $H \to nn$ survives, and the H lifetime would be very long (assuming a typical strong interaction decay width of 100 MeV or $\tau_{strong} \simeq 10^{-23}$ sec, and $\tau_{weak} \gtrsim 10^{-10}$ sec, we might naively expect $\tau_{H\to nn} \gtrsim (\tau_{weak})^2/\tau_{strong} \gtrsim 10^3$ sec, give or take a few orders of magnitude). If m_H < 2130 MeV, the neutral H decays only to neutral particles, and it could not have been seen in emulsion experiments.

To get an idea of how to produce the H, it is useful to note its approximate wave function decomposition (19):

$$\psi_H \gtrsim \sqrt{4/5}\ |8_c \otimes 8_c> + \sqrt{1/10}\ |\Xi N>_{I=0} + \sqrt{1/40}\ |\Lambda\Lambda> + \sqrt{3/40}\ |\Sigma\Sigma>_{I=0}.$$

When grouped into two three-quark states, we see that the H prefers to dissociate into color octets. The most favorable observable channel is ΞN, which enjoys 10% of the probability. An attempt to find the H in the reaction $pp \to K^+K^+H$ was made at Brookhaven (20), but the cross section limits are not very restrictive. The simplest mechanism for this reaction involves two $p \to K^+\Lambda$ dissociations, followed by $\Lambda\Lambda \to H$ recombination. However, the Λ's are in general far off-shell and have a large relative momentum, which is unfavorable for H formation; quasielastic $\Lambda\Lambda$ production is much more likely. A more natural way to produce the H is via the (K^-,K^+) or (K^-,K^0) reactions. Here one brings in one unit of strangeness, which obviates the need for using double associated production. The mechanism for the prototype reaction $^3He(K^-,K^+)Hn$ is shown on the left in Fig. 9. The process $K^-p \to K^+\Xi^-$ is followed by Ξ^-p fusion to form the H. The quasielastic background is generated by the process on the right. Note that ^3He is the simplest target which supplies a diproton; since the pp pair is automatically in a $^1S_0$ state and the $K^-(pp) \to K^+(\Xi^-p)$ reaction has no spin-flip at 0°, the Ξ^-p pair is also a $^1S_0$ and hence in the correct spin state to form an H. In reactions $K^-d \to K^+(\Xi^-n)_{I=1}$ or $K^-d \to K^0(\Xi^-p)_{S=1}$ at 0°, on the other hand, the Ξ^-N pair is prepared with the wrong isospin or spin to become an H.

There are other advantages of the process of Fig. 9 for H production: the elementary 0° cross section for $K^-p \to K^+\Xi^-$ is not small, being about 40 μb/sr at 1.8 GeV/c (see Fig. 2).

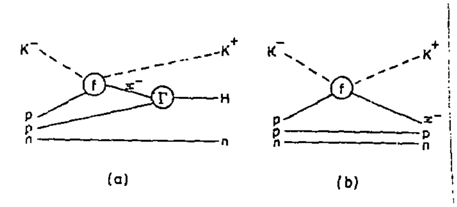

Fig. 9. Reaction mechanism for H production on a ^{3}He target (a); quasielastic background (b)

Also, the Ξ^- recoils with a lab momentum around 400 MeV/c; thus the Ξ^-p relative momentum p_R can be fairly small for protons near the Fermi surface. In calculating the cross section for H formation à la Fig. 9, we (21) have used an expression for the $\Xi^-p \to H$ vertex Γ motivated by the harmonic oscillator quark model: $\Gamma = \Gamma_o \exp(-p_R^2 R_H^2/12)$, where R_H is the bag radius of the H, and Γ_o contains the color-spin-flavor recoupling coefficient and geometrical factors involving the bag radii. This expression for Γ emphasizes the importance of having low p_R to obtain a sizable $\Xi^-p \to H$ fusion probability. For the ^{3}He wave function, we have used a simple product of harmonic oscillator functions in the relative momenta. Plane waves are used for the K^-, K^+, n and H. Preliminary results for the H production cross sections on a ^{3}He target are shown in Figs. 10 and 11. In a missing mass experiment, in which both the K^+ and neutron are detected, the H would show up as a well defined peak which, if m_H is well below the ΛΛ threshold, is nicely separated from the broad quasielastic background. Even if only the K^+ is detected, it should still be possible to see the H, since it shows up as a narrow peak in the K^+ momentum spectrum at 0°. If the H mass is too close to the ΛΛ and Ξ^-p thresholds, however, the signal due to the H may be more difficult to separate from enhancements due to final state interactions. One may also consider heavier targets, which provide more di-proton pairs, but are more subject to distortion effects. The effective number of pp pairs is expected to grow much less rapidly than Z(Z-1), due to absorption (particularly of the K^-), in analogy to the very slow N dependence of the effective neutron number in (K^-,π^-) reactions (22). The $^3He(K^-,K^+n)H$ reaction is the cleanest case, if both K^+ and neutron are detected in coincidence. This experiment is well worth doing: it tests a crucial prediction of the MIT bag model, i.e., the existence of the stable H, and may provide the first definitive example of an n quark state with $n \geq 4$.

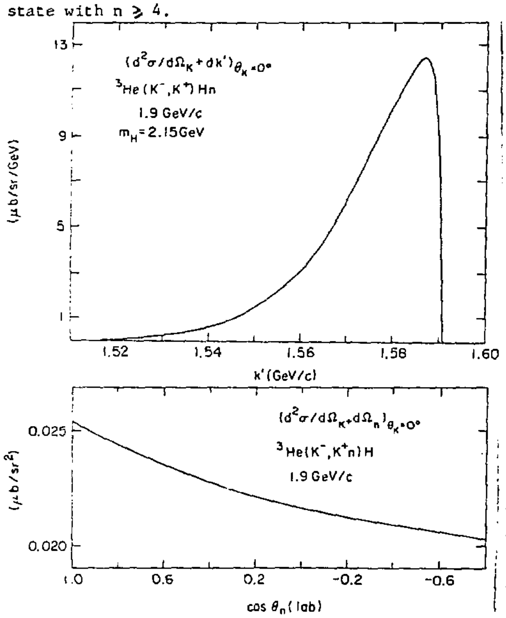

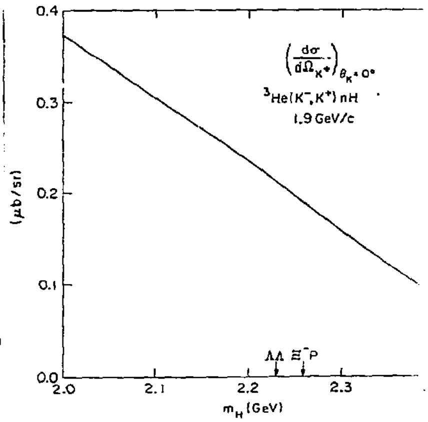

Fig. 10 (left). Differential cross sections for H production on ^{3}He. The upper curve shows the momentum spectrum of the K^+ at 0°; the lower curve gives the neutron angular distribution.

Fig. 11 (above). Differential cross section for H production (only K^+ detected) as a function of the mass of the H.

I would like to thank my collaborators, particularly Ad Aerts, Tony Baltz, Avranam Gal and John Millener, for very helpful comments and discussions. The material discussed here is taken from joint work now in preparation for publication. This research was supported by the U.S. Department of Energy under contract No. DE-AC02-76CH00016.

References

1. B. Povh, Ann. Rev. Nucl. Part. Sci., Eds. J. D. Jackson et al., Vol. 28 (Annual Reviews, Inc., Palo Alto, 1978), p. 1; R. H. Dalitz, Proc. Int. Conf. on Nuclear Physics, Berkeley, 1980, Eds. R. M. Diamond and J. O. Rasmussen (North Holland, Amsterdam, 1981) p. 101.

2. M. Danysz et al., Nucl. Phys. 49, 121 (1963); D. J. Prowse, Phys. Rev. Lett. 17, 782 (1966).

3. A. S. Mondal, A. K. Basak, M. M. Kasim and A. Husain, Nuovo Cim. 54A, 333 (1979); this contains references to earlier work.

4. R. L. Jaffe, Phys. Rev. D15, 267 and 281 (1977); A. T. M. Aerts, Nijmegen Thesis (1979).

5. N. Hoshizaki et al., Prog. Theor. Phys. 60, 1796 (1978) and 61, 129 (1979); W. Grein and P. Kroll, Phys. Lett. 96B, 176 (1980); B. J. Edwards, Phys. Rev. D23, 1978 (1981); objections to the dibaryon interpretation have been given by P. J. Mulders, Phys. Rev. D25, 1269 (1982), W. M. Kloet and R. R. Silbar, Nucl. Phys. A364, 346 (1981), among others.

6. O. Braun et al., Nucl. Phys. B124, 45 (1977).

7. R. L. Jaffe, Phys. Rev. Lett. 38, 195 (1977).

8. R. Bertini et al., Phys. Lett. 90B, 375 (1980); H. Piekarz et al., Phys. Lett. 110B, 428 (1982).

9. C. B. Dover and A. Gal, submitted to Annals of Physics.

10. D. H. Wilkinson et al., Phys. Rev. Lett. 3, 397 (1959); A. Bechdolff et al., Phys. Lett. 26B, 174 (1968); see also ref. 3.

11. C. B. Dover and A. Gal, BNL preprint 30124.

12. M. M. Nagels, T. A. Rijken and J. J. deSwart, Phys. Rev. D20, 1633 (1979); D15, 2547 (1977).

13. A. Gal and C. B. Dover, Phys. Rev. Lett. 44, 379 and 962 (1980).

14. C. B. Dover, Nukleonika 25, 521 (1980).

15. A. J. Baltz, C. B. Dover and D. J. Millener, manuscript in preparation.

16. P. D. Kunz, private communication.

17. D. Marlow et al., Phys. Rev. C25, 2619 (1982).

18. C. B. Dover, unpublished calculations.

19. R. P. Bickerstaff and B. G. Wybourne, J. Phys. G (Nucl. Phys.) 7, 275 (1981); due to a phase error, the H wave function given by these authors contains a spurious $\Sigma^*\Sigma^*$ piece, which should be lumped together with $\Sigma\Sigma$.

20. A. S. Carroll et al., Phys. Rev. Lett. 41, 777 (1978).

21. A. T. M. Aerts and C. B. Dover, manuscript in preparation.

22. R. Bertini et al., Nucl. Phys. A368, 365 (1981).